Supplementary material

Text S1. Analysis of kinetics of mRNA translocation and 30S head rotation by using model proposed by Guo and Noller (2012)

We denote by P_1, P_2, P_3 and P_4 the probabilities of State 1, State 2, State 3 and State 4 shown in Fig. S2a, respectively. Since based on the model State 5 has the same intensity of fluorescence of pyrene dye attached to position +9 of mRNA and the same FRET efficiency between donor Alexa 488 and acceptor Alexa 568 probes attached to position 101 of S11 and position 11 of S13, we can also denote by P_4 the probability of State 5 in Fig. S2a. Based on Fig. S2a, the temporal evolutions of the four probabilities P_1, P_2, P_3 and P_4 are described by the following equations

$$\frac{dP_1(t)}{dt} = -k_1 P_1(t), \tag{S1}$$

$$\frac{dP_2(t)}{dt} = k_1 P_1(t) - k_2 P_2(t), \tag{S2}$$

$$\frac{dP_3(t)}{dt} = k_2 P_2(t) - k_3 P_3(t), \tag{S3}$$

$$\frac{dP_4(t)}{dt} = k_3 P_3(t), \tag{S4}$$

with the initial conditions at t = 0 being as follows: $P_1(0) = 1$ and $P_2(0) = P_3(0) = P_4(0) = 0$. Since rate constant k_1 is much larger than other rate constants, Eqs. (S1) – (S4) can be simplified as

$$\frac{dP_2(t)}{dt} = -k_2 P_2(t), \tag{S5}$$

$$\frac{dP_3(t)}{dt} = k_2 P_2(t) - k_3 P_3(t), \tag{S6}$$

$$\frac{dP_4(t)}{dt} = k_3 P_3(t), \tag{S7}$$

with the initial conditions at t = 0 being as follows: $P_2(0) = 1$ and $P_3(0) = P_4(0) = 0$.

Solving Eqs. (S5) – (S7), we have the following analytical solution

$$P_3(t) = \frac{k_2}{k_2 - k_3}\left(e^{-k_3 t} - e^{-k_2 t}\right), \tag{S8}$$

$$P_4(t) = \frac{k_2}{k_2 - k_3}\left(1 - e^{-k_3 t}\right) - \frac{k_3}{k_2 - k_3}\left(1 - e^{-k_2 t}\right). \tag{S9}$$

With k_2 = 80 s^{-1} and k_3 =10 s^{-1} (see Fig. S2a), from Eq. (S9) we note that $k_2/(k_2-k_3)$ > 0 while $-k_3/(k_2-k_3)$ < 0. Thus, the fluorescence change associated with the mRNA translocation, which is represented by $1-P_4(t)$, cannot be characterized by the sum of two exponentials, whereas it is characterized by one exponential minus another exponential, which is inconsistent with the experimental data of Guo and Noller (2012). The inconsistency can also be seen by comparing Fig. S2b, where we show the results of $P_3(t)$ and $1-P_4(t)$ versus time calculated by using Eqs. (S8) and (S9), with the experimental data [Fig. 2 in Guo and Noller (2012)]. From the comparison it is clearly seen that the theoretical curve for the fluorescence change associated with the mRNA translocation, which is characterized by $1-P_4(t)$ in Fig. S2b, deviates significantly from the experimental curve.

References

Guo Z., Noller H.F., (2012) Rotation of the head of the 30S ribosomal subunit during mRNA translocation. Proc. Natl. Acad. Sci. U.S.A. 109, 20391–20394.

Supporting Figures

(a)

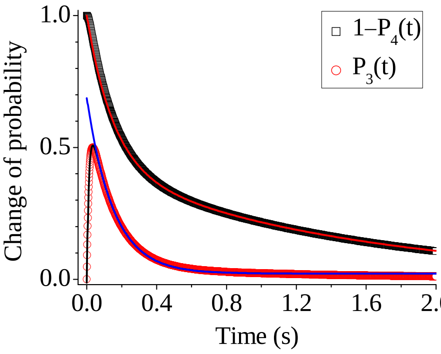

(b)

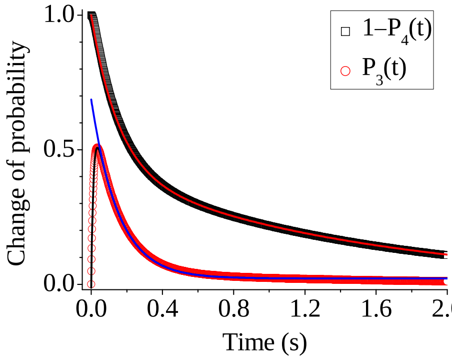

(c)

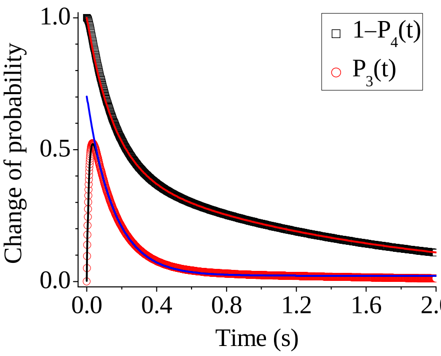

(d)

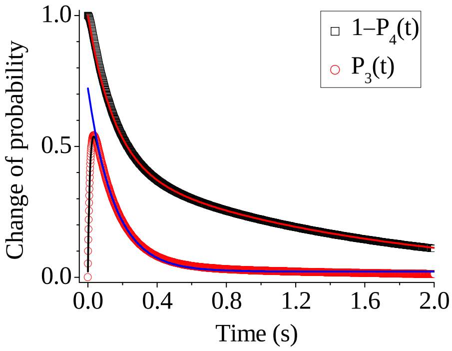

Fig. S1. Temporal evolutions of $P_3(t)$ (open circles) and $1-P_4(t)$ (open squares). **(a)** For the case of fixed k_2 = 0.1 s^{-1}. The data of $P_3(t)$ as a function of t are fit to the function, $P_3(t) = 0.665\exp(-\lambda_3 t) - 0.7\exp(-\lambda_4 t) + 0.022$, where λ_3 = 6.6 s^{-1} and λ_4 = 80 s^{-1} (black line). The data on the slow phase of $P_3(t)$ as a function of t are fit to the single exponential, $P_3(t) = 0.665\exp(-\lambda t) + 0.022$, where λ = 6.6 s^{-1} (blue line). The data of $1-P_4(t)$ are fit to the two-exponential function, $1-P_4(t) = 0.57e^{-\lambda_1 t} + 0.43e^{-\lambda_2 t}$, where λ_1 = 6.6 s^{-1} and λ_2 = 0.69 s^{-1} (red line). **(b)** For the case of fixed k_2 = 0.2 s^{-1}. The data of $P_3(t)$ as a function of t are fit to the function, $P_3(t) = 0.665\exp(-\lambda_3 t) - 0.7\exp(-\lambda_4 t) + 0.022$, where λ_3 = 6.6 s^{-1} and λ_4 = 80 s^{-1} (black line). The data on the slow phase of $P_3(t)$ as a function of t are fit to the single exponential, $P_3(t) = 0.665\exp(-\lambda t) + 0.022$, where λ = 6.6 s^{-1} (blue line). The data of $1 - P_4(t)$ are fit to the two-exponential function, $1 - P_4(t) = 0.57e^{-\lambda_1 t} + 0.43e^{-\lambda_2 t}$, where λ_1 = 6.6 s^{-1} and λ_2 = 0.68 s^{-1} (red line). **(c)** For the case of fixed k_2 = 0.4 s^{-1}. The data of $P_3(t)$ as a function of t are fit to the function, $P_3(t) = 0.68\exp(-\lambda_3 t) - 0.7\exp(-\lambda_4 t) + 0.022$, where λ_3 = 6.5 s^{-1} and λ_4 = 80 s^{-1} (black line). The data on the slow phase of $P_3(t)$ as a function of t are fit to the single exponential, $P_3(t) = 0.68\exp(-\lambda t) + 0.022$, where λ = 6.5 s^{-1} (blue line). The data of $1 - P_4(t)$ are fit to the two-exponential function, $1 - P_4(t) = 0.57e^{-\lambda_1 t} + 0.43e^{-\lambda_2 t}$, where λ_1 = 6.5 s^{-1} and λ_2 = 0.68 s^{-1} (red line). **(d)** For the case of fixed k_2 = 0.6 s^{-1}. The data of $P_3(t)$ as a function of t are fit to the function, $P_3(t) = 0.7\exp(-\lambda_3 t) - 0.7\exp(-\lambda_4 t) + 0.022$, where λ_3 = 6.5 s^{-1} and λ_4 = 80 s^{-1} (black line). The data on the slow phase of $P_3(t)$ as a function of t are fit to the single exponential, $P_3(t) = 0.7\exp(-\lambda t) + 0.022$, where λ = 6.5 s^{-1} (blue line). The data of $1 - P_4(t)$ are fit to the two-exponential function, $1 - P_4(t) = 0.57e^{-\lambda_1 t} + 0.43e^{-\lambda_2 t}$, where λ_1 = 6.5 s^{-1} and λ_2 = 0.67 s^{-1} (red line).

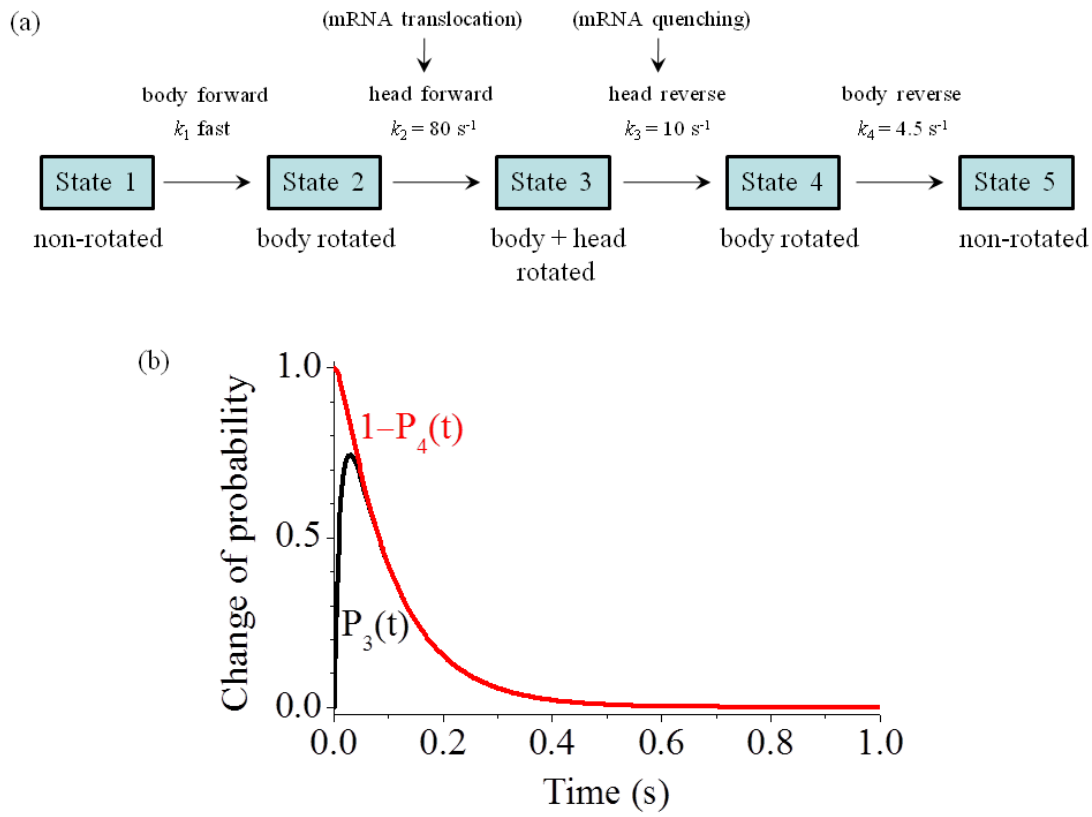

Fig. S2. Kinetics of mRNA translocation and 30S head rotation obtained by using the model for the order of dynamic structural events during mRNA translocation proposed by Guo and Noller (2012). **(a)** The model proposed by Guo and Noller (2012). **(b)** The results of of $P_3(t)$ and $1-P_4(t)$ versus time calculated based on the model shown in (a). $P_3(t)$ corresponds to the fluorescence change associated with the rotation of the 30S head and $1-P_4(t)$ to the fluorescence change associated with the mRNA translocation. Note that the curve of $P_3(t)$ in the slow phase coincides with the curve of $1-P_4(t)$.